Structural and Morphological Control of Mesostructures: Vanadium Based Nanofibers

Zi-Sheng Chao and Eli Ruckenstein*

Department of Chemical Engineering, State University of New York at Buffalo, Amherst, New York 14260

Received March 29, 2002. Revised Manuscript Received August 13, 2002

Mesostructured vanadium−magnesium oxides (V−Mg−O) with various morphologies were synthesized at room temperature using $MgCl_2$ and V_2O_5 as source materials and a large number of surfactants as templates. It was found that, among the surfactants employed, the quaternary ammonium surfactants with long alkyl chains, such as cetyltrimethylammonium bromide (CTAB), or the nonionic surfactant Triton-X 100 could template V−Mg−O mesostructures. In the former case, the synthesized specimen had a lamellar structure and nanofibrous morphology. In the latter case, the specimen had a lamellar structure but a particulate morphology. Among the binary mixtures of cationic, anionic, or nonionic surfactants employed, only the combinations between a quaternary ammonium surfactant and hexadecylamine (HDA) were effective in templating a lamellar mesophase with nanofibrous morphology. The binary surfactants were more effective than the single surfactants in generating a higher regularity of the lamellar mesostructure. Mesostructured V−Mg−O could be synthesized even using binary mixtures consisting of HDA and a quaternary ammonium surfactant with a short alkyl chain, such as benzyltrimethyl (neither of the two was effective when used alone). The mesostructured V−Mg−O nanofibers synthesized with binary mixtures of surfactants were more stable during heating at high temperatures than those synthesized with a cationic surfactant alone.

1. Introduction

The synthesis of mesoporous materials with well-defined structures, templated by supramolecular assemblies of surfactant molecules, has received great attention since their discovery in the early 1990s.[1,2] The driving force for the research activity in this field was provided by the promising applications of these materials to catalysis, selective adsorption−separation, functional materials, chemical sensors, and so forth.[3−11] Depending upon the synthesis conditions, such as the nature of the template employed, the molar ratios of inorganic sources to template, the temperature, the pH, and the reaction time, numerous mesophases have been prepared.[12−21] Silica was employed to synthesize the hexagonal MCM-41,[2] the cubic MCM-48,[2,22] and the lamellar MCM-50.[23] Non-silica oxides or their combinations have also been used as sources for the preparation of mesoporous materials.

Among the various non-silica-based mesoporous materials, those containing vanadium are important because of the unique catalytic applications of vanadium-based oxides in the selective oxidation of hydrocarbons. Several papers have been concerned with the synthesis

* Corresponding author. Telephone: (+1-716) 6452911/2214. Fax: (+1-716) 6453822. E-Mail: feaeliru@acsu.buffalo.edu.

(1) Kresge, C. T.; Leonowicz, M. E.; Roth, W. J.; Vartuli, J. C.; Beck, J. S. *Nature* **1992**, *359*, 710.
(2) Beck, J. S.; Vartuli, J. C.; Roth, W. J.; Leonowicz, M. E.; Kresge, C. T.; Schmitt, K. D.; Chu, C. T. W.; Olson, D. H.; Sheppard, E. W.; McCullen, S. B.; Higgins, J. B.; Schlenker, J. L. *J. Am. Chem. Soc.* **1992**, *114*, 10834.
(3) Barton, T. J.; Bull, L. M.; Klemperer, W. G.; Loy, D. A.; McEnaney, B.; Misono, M.; Monson, P. A.; Pez, G.; Scherer, G. W.; Vartuli, J. C.; Yaghi, O. M. *Chem. Mater.* **1999**, *11*, 2633.
(4) Ma, Y.; Tong, W.; Zhou, H.; Suib, L. A. *Microporous Mesoporous Mater.* **2000**, *37*, 243.
(5) Cheetham, A. K.; Ferey, G.; Loiseau, T. *Angew. Chem., Int. Ed. Engl.* **1999**, *38*, 3269.
(6) Behrens, P. *Adv. Mater.* **1993**, *5*, 127.
(7) Sayari, A. *Chem. Mater.* **1996**, *8*, 1840.
(8) Corma, A. *Chem. Rev.* **1997**, *97*, 2373.
(9) Brunel, D. *Microporous Mesoporous Mater.* **1999**, *27*, 329.
(10) Ying, J. Y.; Mehnert, C. P.; Wong, M. D. *Angew. Chem., Int. Ed.* **1999**, *38*, 56.
(11) Selvam, P.; Bhatia, S. K.; Sonwane, C. G. *Ind. Eng. Chem. Res.* **2001**, *40*, 3237.
(12) Raman, N. K.; Anderson, M. T.; Brinker, C. J. *Chem. Mater.* **1996**, *8*, 1682.
(13) Huo, Q.; Margolese, D. I.; Ciesla, U.; Demuth, D. G.; Feng, P.; Gier, T. E.; Sieger, P.; Firouzi, A.; Chmelka, B. F.; Schuth, F.; Stucky, G. D. *Chem. Mater.* **1994**, *6*, 1176.
(14) Sakamoto, Y.; Kaneda, M.; Terasaki, O.; Zhao, D. Y.; Kim, L. M.; Stucky, G. D.; Shin, H. J.; Ryoo, R. *Nature* **2000**, *408*, 449.
(15) Huo, Q.; Leon, R.; Petroff, P. M.; Stucky, G. D. *Science* **1995**, *268*, 1324.
(16) Zhao, D. Y.; Huo, Q.; Feng, J. L.; Chmelka, B. F.; Stucky, G. D. *J. Am. Chem. Soc.* **1998**, *120*, 6024.
(17) Zhao, D. Y.; Huo, Q.; Feng, J. L.; Kim, J.; Han, Y.; Stucky, G. D. *Chem. Mater.* **1999**, *11*, 2668.
(18) Tanev, P. T.; Pinnavaia, T. J. *Science* **1995**, *267*, 865.
(19) Bagshav, S. A.; Prouzet, E.; Pinnavaia, T. J. *Science* **1995**, *269*, 1242.
(20) Kim, S. S.; Zhang, W.; Pinnavaia, T. J. *Science* **1998**, *282*, 1302.
(21) Ryoo, R.; Kim, J. M.; Shin, C. H.; Lee, J. Y. *Stud. Surf. Sci. Catal.* **1996**, *105A*, 45.
(22) Monnier, A.; Schuth, F.; Huo, Q.; Kumar, D.; Margolese, D.; Maxwell, R. S.; Stucky, G. D.; Krishnamurty, M.; Petroff, P.; Firouzi, A.; Janicke, M.; Chmelka, B. F. *Science* **1993**, *261*, 1299.
(23) Vartuli, J. C.; Kresge, C. T.; Roth, W. J.; McCullen, S. B.; Beck, J. S.; Schmitt, K. D.; Leonowicz, M. E.; Lutner, J. D.; Sheppard, E. W. In *Proceedings of the 209th ACS National Meeting, Division of Petroleum Chemistry*; American Chemical Society: Washington, DC, 1995; pp 21−25.

10.1021/cm020127i CCC: $22.00
Published on Web 09/19/2002

of vanadium oxide, vanadium-doped silicate, and alumino-phosphoro-vanadate mesoporous materials.[24−32] Recently, Yagi et al.[33] examined the transformations of mesoporous vanadium oxide templated by hexadecyltrimethylammonium surfactant, which occur during low-temperature calcination. They observed that the lamellar mesostructure was transformed to other mesophases during calcination at 433 K and that the mesostructures were stable below 523 K.

In the present paper, vanadium(V) oxide and magnesium chloride were used as source materials to synthesize mesostructured V−Mg−O. The nanofibrous morphology obtained in some cases was not observed previously when the vanadium source was vanadium acetylacetonate ($V(acac)_3$).[34] Most importantly, the synthesized mesostructured V−Mg−O's were more stable than the mesostructured vanadium reported by Yagi.[33] This opens the possibility to improve the stability of this mesoporous material by introducing magnesium into the vanadium framework.

2. Experimental Section

2.1. Reagents. The reagents were purchased from Aldrich and used without further purification. Vanadium(V) oxide and magnesium chloride were used as sources for V and Mg. The surfactants employed as templates can be divided into four classes: (I) cationic surfactants (benzyltrimethylammonium bromide (BTAB), cetylpyridium bromide (CPB), cetyltrimethylammonium bromide (CTAB), dodecyltrimethyammonium bromide (DTAB), myristyltrimethylammonium bromide (MTAB), hexamine, octamine, hexadecylamime (HDA), octadecylamine, and eicosylamine); (II) anionic surfactants (sodium dodecyl sulfate (SDS), sodium dodecylbenzene sulfonate (SDBS), and sodium dioctyl sulfosuccinate (SDSS)); (III) nonionic surfactants (Triton X-100, Span 65, Brij 35, Brij 96, Tween 20, Tween 40, triblock copolymers poly(ethylene oxide)−poly(propylene oxide)−poly(ethylene oxide) (PEO−PPO−PEO), poly(ethylene glycol), poly(propylene glycol), poly(ethylene oxide) diamine terminated, poly(propylene oxide) diamine terminated, poly(4-vinylpyridine-*co*-butyl methacrylate), and poly(butadiene)-diol); and (IV) equimolar binary mixtures of surfactants of classes I and II, or equimolar mixtures of surfactants of a primary amine and a quaternary ammonium salt of class I.

2.2. Synthesis. The synthesis of the mesostructured V−Mg−O was carried out using the following steps: (i) vanadium(V) oxide was dissolved into an aqueous solution of sodium hydroxide (molar ratio $NaOH/V_2O_5 = 2$) with stirring and heating at the boiling point; (ii) magnesium chloride and the surfactants were dissolved into an aqueous solution of hydrochloric acid (molar ratio $HCl/V_2O_5 = 2$) with vigorous stirring at room temperature (For the nonionic surfactants, a suitable amount of ethanol had to be introduced to increase their solubility.); (iii) the first solution was slowly added to the second one with vigorous stirring at room temperature, resulting in a mixture with the molar composition

$$1.0\ V_2O_5/1.0\ MgCl_2/0.25\ \text{surfactant}/295\ H_2O/x\ \text{ethanol}$$

where $x = 0$ for the cationic and anionic surfactants and $x = 18$ for the nonionic ones. The above mixture had a pH of 3−4 and was stirred for 24 h to yield a homogeneous slurry, which was then allowed to age at room temperature for 2 days. The solid product was recovered by filtration, washed with distilled water, and dried at 373 K for 12 h.

2.3. Characterization. The X-ray diffraction (XRD) patterns were obtained with a SIEMENS D500 diffractometer using Cu Kα radiation of wavelength 1.5406 Å. The diffraction data were recorded for 2θ angles between 1° and 15°, with a resolution of 0.02°.

Transmission electron microscopy (TEM) and selected area electron diffraction (SAED) were carried out using a JEM-2010 electron microscope equipped with a tungsten gun operating at an accelerating voltage of 200 KV. Before the TEM measurements, the specimens were ground in methanol and supported on a holey carbon film located on a Cu grid.

Nitrogen adsorption−desorption isotherms were obtained at 77 K with a Micromeritics ASAP 2010 Gas Sorption and Porosimetry instrument. The synthesized specimens were first heated in a flow of nitrogen from room temperature up to 623 K at a heating rate of 10 K/min, and they were kept at 623 K for 8 h in order to remove the surfactant. The specimens were then located in an ASAP 2010 apparatus and outgassed at 623 K for 4 h under a vacuum of 1×10^{-3} Torr. The specific surface area was determined by the BET method, and the pore volume was calculated at a relative pressure of $P/P_0 > 0.99$, assuming full surface coverage with nitrogen. The pore size distribution was obtained from the N_2 desorption branch by the BJH (Barrett−Joyner−Halenda) method.

The chemical composition of the samples was determined using a Perkin-Elmer model AAS 3030 spectrophotometer. The specimens were first calcined at 873 K in air for 4 h to completely remove the organic surfactants and then digested in a mixed solution of nitric acid and muriatic acid using a LEM MOS2000 Microwave Digester. Magnesium and vanadium were determined using an acetylene/air and an acetylene/nitrous oxide flame atomic absorption spectrophotometer at wavelengths of 285.2 and 318.4 nm, respectively.

3. Results and Discussion

3.1. Synthesis of Mesostructured V−Mg−O with Single Surfactants. Many surfactants are effective in templating silica mesophases. For example, the alkyltrimethylammonium ions with long alkyl chains could template hexagonal mesophases, the triblock copolymers PPO−PEO−PPO cubic mesophases, and Triton X-100 lamellar mesophases. We employed the above popular surfactants and many other surfactants listed in the Experimental Section to synthesize mesostructured V−Mg−O's. It was found that the anionic surfactants (class II) and the amines among the cationic surfactants (class I) could not template any V−Mg−O mesophase; most of the nonionic surfactants (class III), such as the alcohols, ethers, or esters, with long alkyl chains were also inactive. These findings were provided by the X-ray diffraction patterns, which exhibited no characteristic diffraction peaks for 2θ angles between 1.5 and 15°. An exception was the nonionic surfactant Triton X-100, which could template a mesostructured V−Mg−O. Figure 1A presents its XRD pattern and shows that the specimen exhibited equidistanced diffraction peaks at $2\theta = 3.08$, 6.28, 9.48, and 12.68°, indicating a typical lamellar structure. Besides the above peaks, there are also some weak peaks at $2\theta =$ 10−11°, which were probably caused by a nonindexed

(24) Luca, V.; Hook, J. M. *Chem. Mater.* **1997**, *9*, 2731.
(25) Tuel, A. *Microporous Mesoporous Mater.* **1999**, *27*, 151.
(26) Vansant, E. F. *J. Catal.* **2001**, *197*, 160.
(27) Dai, L. X.; Tabata, K.; Suzuki, E. *J. Mater. Sci. Lett.* **2000**, *19*, 2071.
(28) Dai, L. X.; Tabata, K.; Suzuki, E.; Tatsumi, T. *Chem. Mater.* **2001**, *13*, 208.
(29) Morey, M. S.; Davidson, A.; Stucky, G. D. *J. Porous Mater.* **1998**, *5*, 195.
(30) Gougeon, R. D.; Bodart, P. R.; Harris, R. K.; Kolonia, D. M.; Petrakis, D. E.; Pomonis, P. J. *Phys. Chem. Chem. Phys.* **2000**, *2*, 5286.
(31) Kolonia, K. M.; Petrakis, D. E.; Angelidis, T. N.; Trikalitis, P. N.; Pomonis, P. J. *J. Mater. Chem.* **1997**, *7*, 1925.
(32) Mizuno, N.; Hatayama, H.; Uchida, S.; Taguchi, A. *Chem. Mater.* **2001**, *13*, 179.
(33) Yagi, Y.; Zhou, H.; Miyayama, M.; Kudo, T.; Honma, I. *Langmuir* **2001**, *17*, 1328.
(34) Chao, Z. S.; Ruckenstein, E. *Langmuir* **2002**, *18*, 734.

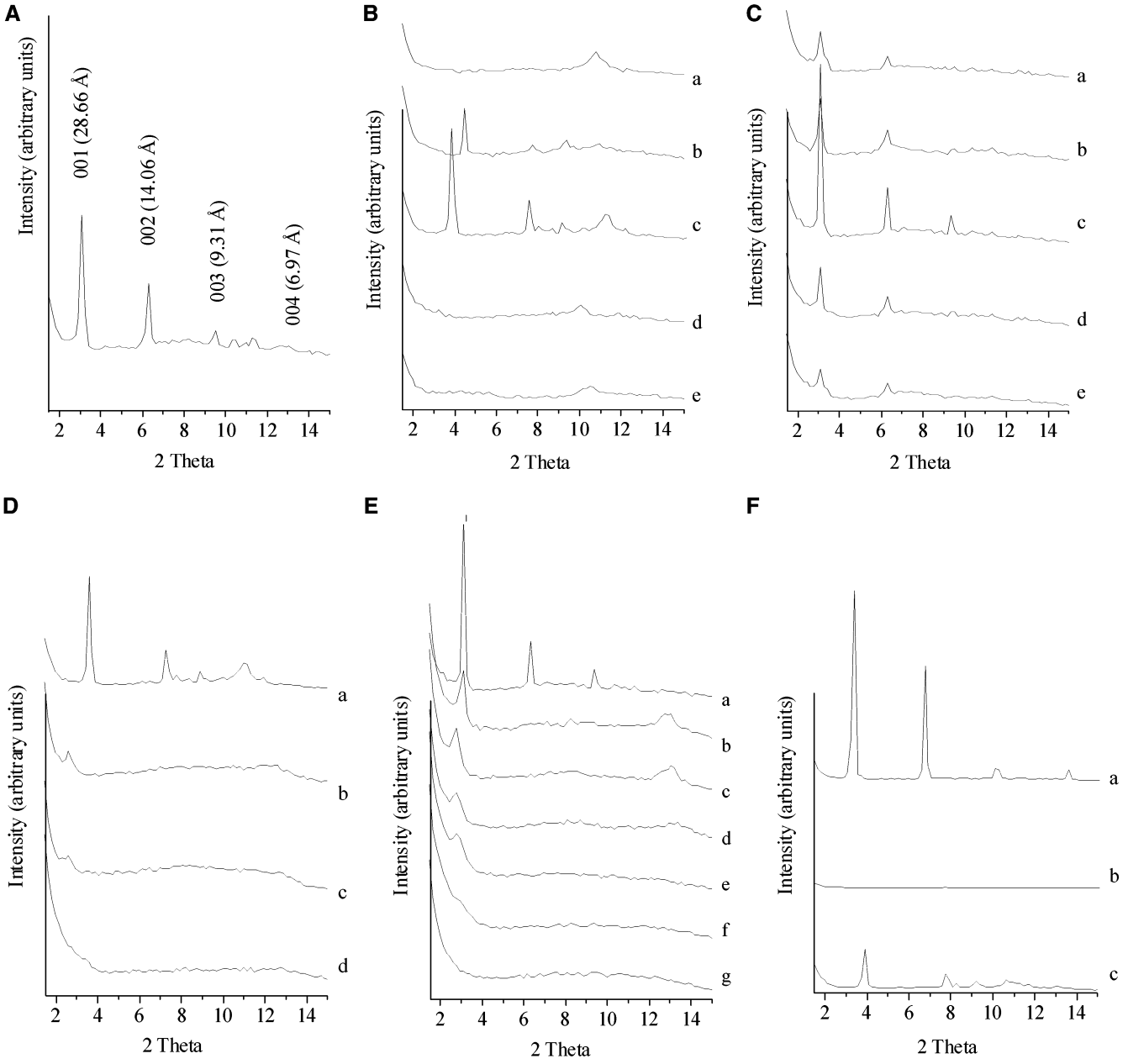

Figure 1. (A) XRD pattern of the as-synthesized mesostructured V−Mg−O prepared with Triton X-100. (B) XRD patterns of the as-synthesized mesostructured V−Mg−O's prepared with various quaternary ammonium bromide surfactants: (a) benzyltrimethylammonium bromide (BTAB); (b) cetylpyridium bromide (CPB); (c) cetyltrimethylammonium bromide (CTAB); (d) dodecyltrimethylammonium bromide (DTAB); (e) myristyltrimethylammonium bromide (MTAB). (C) XRD patterns of the as-synthesized mesostructured V−Mg−O's prepared with binary mixtures of surfactants, consisting of hexadecylamine (HDA) and (a) benzyltrimethylammonium bromide (BTAB), (b) cetylpyridium bromide (CPB), (c) cetyltrimethylammonium bromide (CTAB), (d) dodecyltrimethylammonium bromide (DTAB), or (e) myristyltrimethylammonium bromide (MTAB). (D) XRD patterns of the mesostructured V−Mg−O's synthesized with CTAB. Before the spectra were recorded, the specimens were pretreated by calcination in a flow of Ar at various temperatures for 2 h: (a) 373 K; (b) 423 K; (c) 523 K; (d) 623 K. (E) XRD patterns of a mesostructured V−Mg−O's synthesized with CTAB + HDA. Before the spectra were recorded, the specimens were pretreated by calcination in a flow of Ar at various temperatures for 2 h: (a) 373 K; (b) 423 K; (c) 473; (d) 523 K; (e) 573 K; (f) 623 K; (g) 673 K. (F) XRD patterns of (a) powder CTAB, (b) powder V_2O_5, and (c) mesostructured vanadium oxide prepared with CTAB.

compound between V, Mg, and O. The chemical compositions of the specimens are listed in Table 1.

The same specimen was also examined by transmission electron microscopy and selected area electron diffraction (Figure 2). An ordered lamellar structure can be observed, consisting of gray−black-alternating layers. The black layers represent the inorganic ones composed of V, Mg, and O, and the gray layers the space between them. For the average distance between layers and the thickness of the layers, the values 2.15 and 0.71 nm, respectively, could be determined. The SAED patterns contain two small spots located in line at the same distance from a central large spot, confirming the ordered mesostructure of the specimen.

We also examined the textural properties of the Triton X-100-based specimen by N_2 adsorption−desorption, and the results are presented in Figure 3. One can see that the N_2 adsorption−desorption isotherm belongs to type IV, according to the IUPAC classification, with a hysteresis loop specific to mesoporous materials. The

Table 1. Chemical Compositions of the Specimens Prepared with Different Surfactants[a]

surfactant	atomic ratio of V/Mg
Triton X-100	53.25
BTAB	21.59
CPB	35.29
CTAB	39.24
MTAB	44.49
DTAB	35.74
BTAB + HDA	16.83
CPB + HDA	20.58
CTAB + HDA	24.17
MTAB + HDA	26.85
DTAB + HDA	26.22

[a] The specimens were calcined in air at 873 K for 4 h before being used in the atomic absorption spectrophotometric analysis.

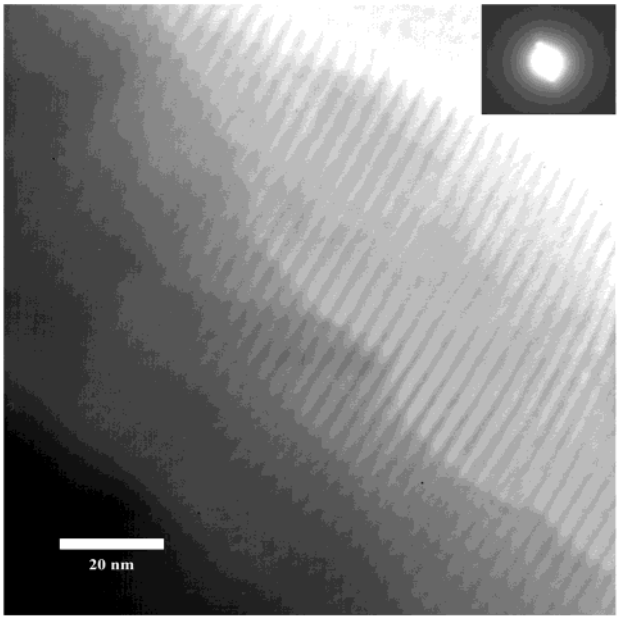

Figure 2. Transmission electron micrograph and selected area electron diffraction pattern of the as-synthesized mesostructured V−Mg−O prepared with Triton X-100.

specific surface area, the pore volume, and the average pore size are 232 m^2/g, 0.32 cm^3/g, and 5.46 nm, respectively. The pore size distribution curve shows that the pore sizes of most mesopores are in a narrow range.

Among the cationic surfactants (class I), the quaternary ammonium salts with various lengths of their alkyl chains (e.g., BTAB, CPB, CTAB, DTAB, and MTAB) were used in the synthesis of mesostructured V−Mg−O. The chemical compositions of these specimens are listed in Table 1. The XRD indicated that only the specimens prepared with CPB (Figure 1B,b) and CTAB (Figure 1B,c) exhibited lamellar mesostructures, with almost equidistant diffraction peaks. The *d* spacings of these two specimens are listed in Table 2. However, the specimens prepared with the surfactants BTAB, DTAB, or MTAB exhibited either very weak or no peaks specific to mesostructures in the low 2θ range, and only one broad peak in the higher 2θ range.

The morphology and structure of the specimens prepared with various quaternary ammonium surfactants were examined by TEM and SAED, and the micrographs and the diffraction patterns are presented in Figure 4. All the specimens have (at least in part) a fibrous morphology; those prepared with CPB (Figure 4a) and CTAB (Figure 4b) possess almost exclusively a fibrous lamellar structure with high crystallinity, while those prepared with BTAB, DTAB, and MTAB (not shown) contained also an amorphous phase. The TEM micrographs also provided the distance between layers and their thickness, and the results are listed in Table 2. The specimen templated by CTAB possesses the largest distance between layers, and the results obtained via XRD and TEM are in agreement. One can conclude that the quaternary ammonium surfactants containing long alkyl chains can template mesoporous V−Mg−O's, and the longer the alkyl chain, the higher is the crystallinity, and the larger the distance between layers. It should be noted that vanadium oxide nanotubes and fibers have been also obtained in refs. 35 and 36, respectively.

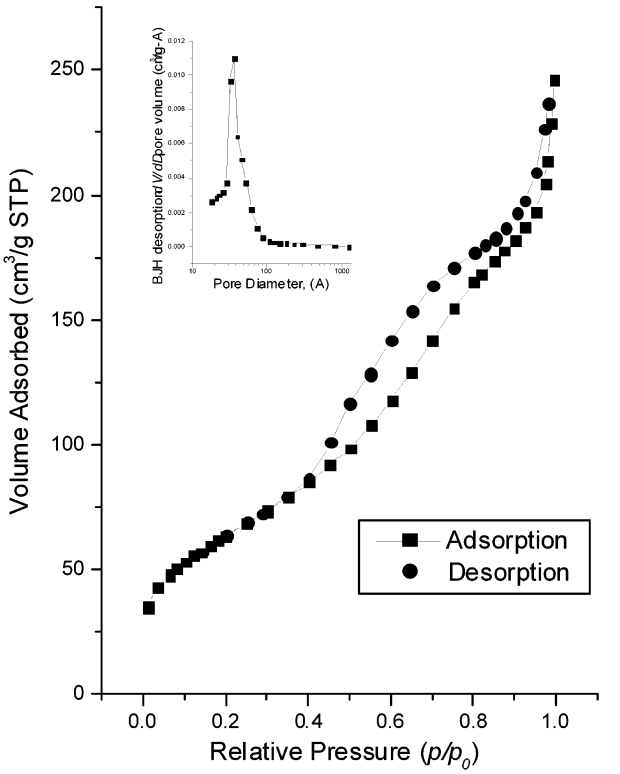

Figure 3. N_2 adsorption−desorption isotherm and pore size distribution of mesostructured V−Mg−O synthesized with Triton X-100.

Table 2. *d* Spacings of Mesostructured V−Mg−O Prepared with Different Quaternary Ammonium Surfactants

	TEM		XRD
surfactant	distance between layers (nm)	layer thickness (nm)	*d*-spacing (nm)
BTAB	0.66	0.16	
CPB	1.56	0.40	1.97
CTAB	1.70	0.60	2.28
MTAB	0.69	0.21	
DTAB	0.64	0.21	

The SAED patterns (Figure 4) exhibit a long range ordering, since sharp reflection spots extend over 3−4 orders. The patterns consist of spots arranged in a

(35) Niederberger, M.; Muhr, H.-J.; Krumeich, F.; Bieri, F.; Günther, D.; Nesper, R. *Chem. Mater.* **2000**, *12*, 1995.
(36) Ruckenstein, E.; Chao, Z.-S. *Nanoletters*, **2001**, *1*, 739.

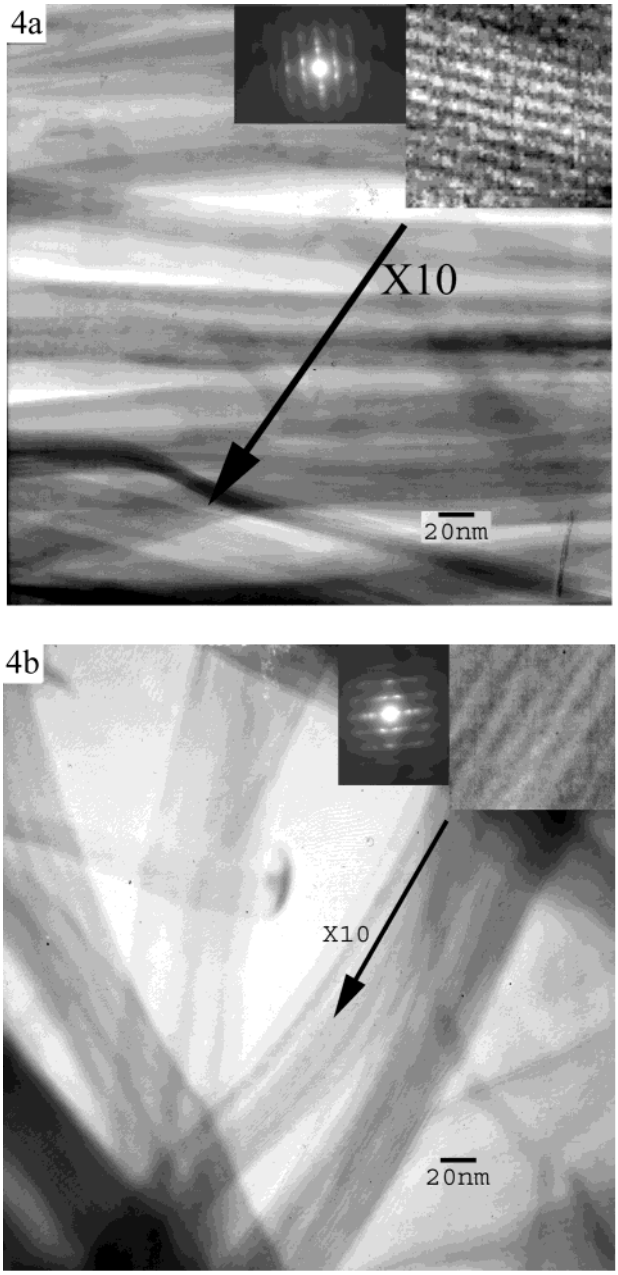

Figure 4. Transmission electron micrographs and selected area electron diffraction of as-synthesized mesostructured V−Mg−O's prepared with quaternary ammonium bromide surfactants: (a) cetylpyridium bromide (CPB); (b) cetyltrimethylammonium bromide (CTAB). The inset in the right corner magnifies the region indicated by the arrow by a factor of 10.

matrix, indicating that the specimens have a lamellar structure with an ordering within the layer itself.

The textural properties of the specimens prepared with the quaternary ammonium surfactants were investigated via N_2 adsorption−desorption experiments, and two of the isotherms and pore size distributions are presented in Figure 5. One can see that the isotherms are of type IV and exhibit the characteristic hysteresis loop of mesostructured materials. The starting points of the hysteresis loops for the specimens prepared with CPB and CTAB are at about $P/P_0 = 0.4$, and for the specimens prepared with BTAB, DTAB, and MTAB they are at about $P/P_0 = 0.3$. Table 3 lists the textural properties of the specimens. The specimens prepared with CPB and CTAB had higher specific surface areas

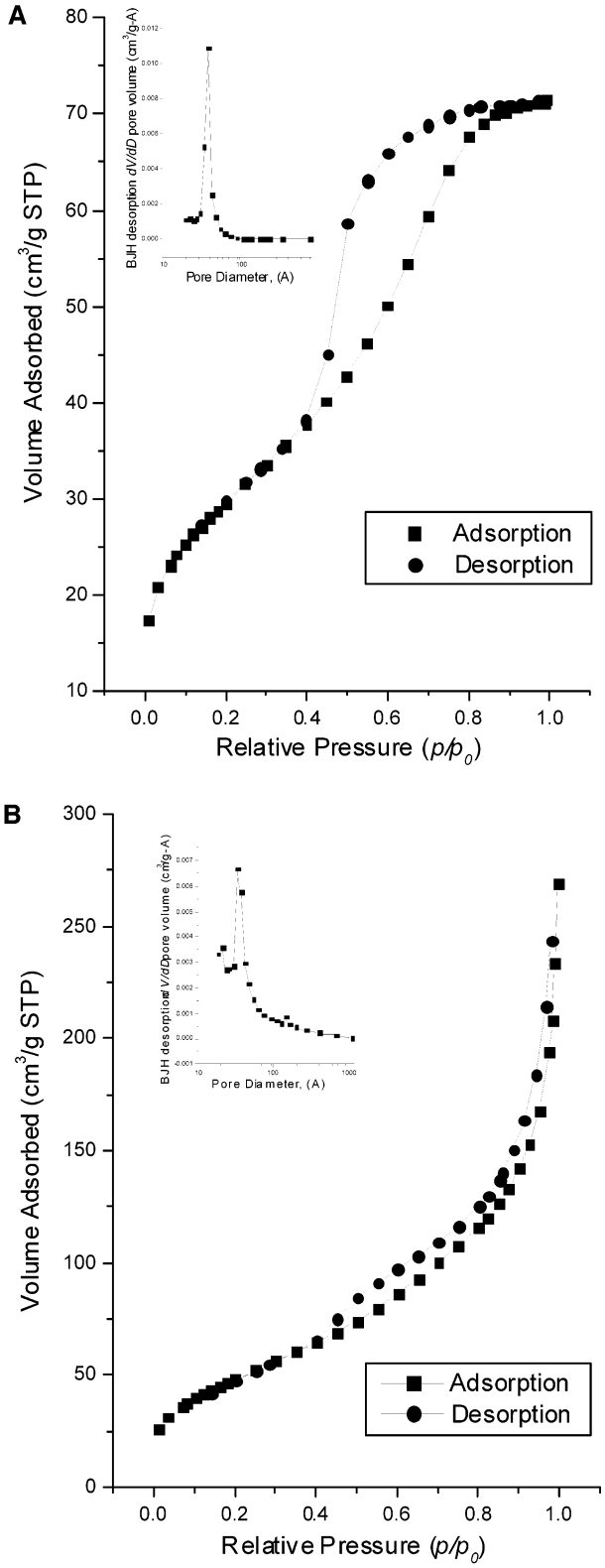

Figure 5. N_2 adsorption−desorption isotherms and pore size distributions of V−Mg−O's synthesized with a quaternary ammonium bromide surfactant: (a) cetylpyridium bromide (CPB) and (b) cetyltrimethylammonium bromide (CTAB).

and pore volumes. This indicates that the larger the alkyl chain of the quaternary ammonium surfactant, the greater the tendency for the formation of a mesostructured V−Mg−O. It should be noticed that the average pore sizes obtained via N_2 adsorption are much larger than the distance between layers determined via XRD

Table 3. Textural Properties of Mesostructured V−Mg−O Prepared with Various Quaternary Ammonium Surfactants

surfactant	specific surface area (m^2/g)	pore volume (cm^3/g)	average pore size (nm)
BTAB	14.6	0.02	5.29
CPB	106.6	0.11	4.12
CTAB	178.0	0.30	6.70
MTAB	61.5	0.12	7.82
DTAB	62.7	0.097	6.05

and TEM. This occurred because of the thermal pretreatment of the specimens before the N_2 adsorption experiments.

3.2. Synthesis of Mesostructured V−Mg−O with Binary Mixtures of Surfactants. The binary mixtures between the surfactants of class I (primary amines and quaternary ammonium salts) and class II (DBSS, SDBS, and DSS) were inactive in templating V−Mg−O mesostructures. Evidence in this direction was brought by the XRD patterns, which were free of the peaks specific to mesoporous materials. Mesostructured V−Mg−O's could be, however, synthesized with binary mixtures consisting of an amine surfactant and a quaternary ammonium surfactant. Figure 1C presents the XRD patterns of the specimens prepared with mixtures consisting of hexadecylamine (HDA) and a quaternary ammonium surfactant (BTAB, CTAB, CPB, DTAB, or MTAB). The almost equidistanced diffraction peaks in the 2θ angles indicated that the specimens have lamellar structures. Their *d* spacings were almost independent of the nature of the quaternary ammonium surfactants employed, and very near to 2.86 nm. Since hexadecylamine alone failed to template a mesostructured V−Mg−O and only CTAB and CPB among the quaternary ammonium surfactants could template such a mesophase, one can conclude that there is a synergistic cooperation between the two surfactants. One can also notice that there are some weak peaks for 2θ values between 9 and 13°, which are probably caused by some nonindexed compounds between V, Mg, and O. The compositions of these specimens are listed in Table 1, which shows that the V/Mg atomic ratios for the binary surfactants are lower than those for the single surfactants.

Figure 6 presents the TEM micrographs of the specimens based on mixtures of HDA and a quaternary ammonium surfactant. All of them have a fibrous morphology with fibers of an average diameter of about 50 nm and a length of over 1000 nm. Under a higher resolution, one could observe that the fibers are composed of numerous layers, which have an average thickness of about 0.6 nm, separated by distances of 2.25 nm, again independent of the nature of the quaternary ammonium surfactant employed. The sums of the average thickness and the separation distance coincide with the XRD *d* spacings. Figure 6 also contains the SAED patterns of the specimens, which are similar to those prepared with the corresponding single surfactants (Figure 4). They again indicate a lamellar structure with an ordering within the layers themselves.

Figure 7 presents the N_2 adsorption−desorption isotherms and the pore size distribution of the specimens templated by some of the mixtures of HDA and a quaternary ammonium surfactant. The textural properties of these specimens are listed in Table 4. As the

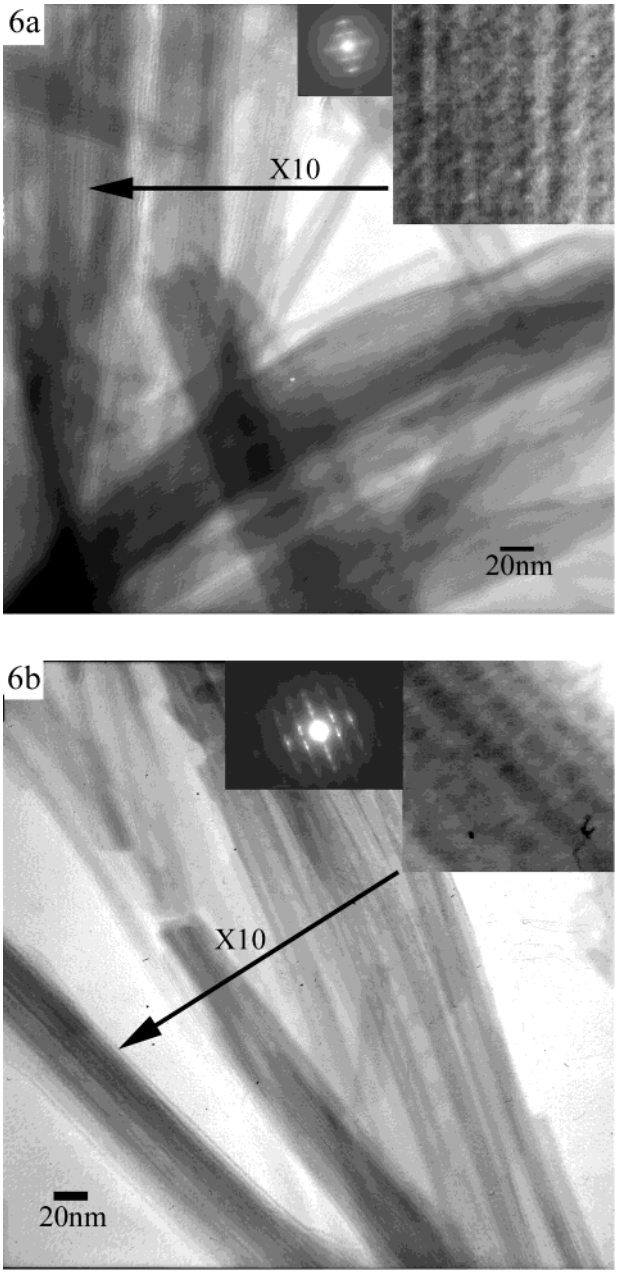

Figure 6. Transmission electron micrographs and selected area electron diffraction patterns of as-synthesized mesostructured V−Mg−O's prepared with binary mixtures of surfactants, consisting of hexadecylamine (HAD) and (a) cetylpyridium bromide (CPB) and (b) cetyltrimethylammonium bromide (CTAB). The inset in the right corner magnifies the region indicated by the arrow by a factor of 10.

length of the alkyl chain in the quaternary ammonium ions increases, the specific surface area and the pore volume of the specimen increase. The average pore sizes of the specimens obtained via N_2 adsorption are larger than the distance between layers in the lamellar structure obtained via XRD and TEM for reasons explained before.

3.3. Stability of the Mesostructured V−Mg−O. The stability of the mesostructured V−Mg−O was investigated by XRD and N_2 adsorption using specimens prepared with a single surfactant (CTAB) and a binary mixture (CTAB + HDA). The as-synthesized specimens were heated from room temperature to a selected one at a rate of 5 K/min in a flow of argon and kept at that

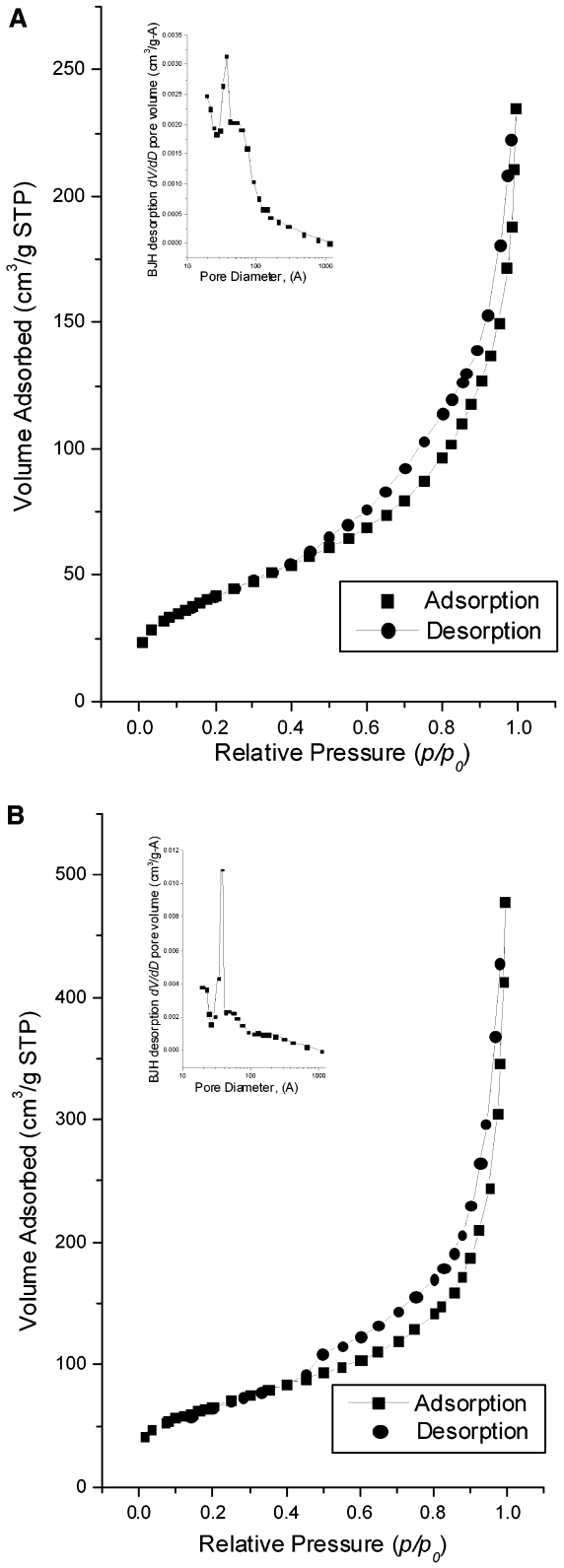

Figure 7. N_2 adsorption−desorption isotherms and pore size distributions of mesoporous V−Mg−O's synthesized with binary mixtures of surfactants, consisting of hexadecylamine (HDA) and (a) cetylpyridium bromide (CPB) and (b) cetyltrimethylammonium bromide (CTAB).

temperature for 2 h. Then the specimens were characterized by XRD or used in N_2 adsorption experiments. Figure 1D presents the XRD patterns of the specimen based on CTAB, calcined at various temperatures. One can see that after the specimen was calcined at 423 K

Table 4. Textural Properties of Mesostructured V−Mg−O's Prepared with Binary Mixtures Composed of Various Quaternary Ammonium Ions and HDA

surfactant	specific surface area (m^2/g)	pore volume (cm^3/g)	average pore size (nm)
BTAB + HDA	113.1	0.20	7.17
CPB + HDA	151.9	0.37	9.2
CTAB + HDA	237.7	0.45	7.56
MTAB + HDA	148.0	0.25	6.68
DTAB + HDA	106.5	0.22	8.24

(Figure 1D,b), the characteristic peaks of the lamellar mesophase disappeared. However, a new peak appeared at an even lower angle than that for the main peak of the lamellar structure. This indicates that the lamellar phase was transformed into a distorted hexagonal or wormlike one, with a pore size larger than the distance between the layers. When the temperature was increased to 523 K (Figure 1D,c), the peak decreased in intensity and broadened toward a lower angle. When the temperature was increased above 623 K (Figure 1D,d), the peak could hardly be observed, probably because its diffraction at small angle was screened by the strong background scattering and/or has a too low intensity. Hence, with increasing temperature, the surfactants were gradually removed and the layers rearranged, generating large pores. A similar behavior was also observed with the specimen prepared with CTAB + HDA. As shown in Figure 1E, with increasing calcination temperature, the specific diffraction peaks of the lamellar mesophase disappeared, and those of a distorted hexagonal or wormlike phase appeared at a lower 2θ than that for the lamellar phase. It should be noticed that the specimen prepared with CTAB + HDA was more stable than that prepared with the single surfactant (CTAB), because some crystallinity survived at 573 K in the former case but was lost in the latter one. Additional evidence in the same direction was brought by the N_2 adsorption experiments. When the specimen based on the single surfactant CTAB was pretreated in a flow of N_2 at 623 K for 6 h, followed by vacuum treatment for 10 h at the same temperature, the specific surface area, pore volume, and average pore size were 178 m^2/g, 0.30 cm^3/g, and 6.7 nm, respectively. When another specimen prepared with CTAB was pretreated in a flow of N_2 at 673 K for 7 h, followed by vacuum treatment for 12 h at the same temperature, the specific surface area and pore volume decreased to 87 m^2/g and 0.20 cm^3/g, respectively, and the average pore size increased to 8.96 nm. This means that 48.9% of the specific surface area and 65.0% of the pore volume remained after the treatment at the higher temperature for a longer time. The same experiment was also conducted with specimens based on CTAB + HAD. It was found that the specific surface area and the pore volume decreased from 238 m^2/g and 0.45 cm^3/g to 136 m^2/g and 0.33 cm^3/g, respectively, and the average pore size increased from 7.6 to 9.7 nm. In this case, the final specific surface area and volume were 57.1% and 73.3% of the first, respectively. The higher stability of the specimen prepared with the binary mixture CTAB + HDA might be due to the higher magnesium content (lower V/Mg atomic) ratio (see Table 1) in the specimen based on the binary surfactant mixture. A detailed study of the stability of the mesostructured V−Mg−O has shown that the stability was strongly dependent on the

magnesium content in the mesophase (which is controlled by pH) and the procedure employed to remove the surfactant from the mesophase. The examination of the results will be reported in a separate paper.

3.4. Mechanism for the Formation of Mesostructured V−Mg−O's. The similarity between the liquid crystal surfactant assemblies and M41S suggested a "liquid crystal templating" (LCT) mechanism[2] for the formation of a mesophase from an anionic silicate species and a cationic surfactant (CTAB). One possible pathway assumed the presence of a liquid-crystal mesophase prior to the addition of the inorganic reagents, that is, the preexistence of surfactant aggregates (rodlike micelles), followed by the polymerization of the silicate anions within the preexisting structures, resulting in the formation of the MCM-41. Another possible pathway assumed the formation of a liquid-crystal structure from the ion pairs between the silicate anions and the surfactant cations in solution. In both pathways, the inorganic components that are negatively charged were considered to interact with the positively charged ammonium headgroups of the surfactants and to condense together into a solid framework. The details of the MCM-41 formation have not yet been fully identified. We are inclined to believe that both mechanisms can occur. For instance, when V_2O_5 alone was used to prepare a mesostructured vanadium oxide and CTAB was employed as surfactant, probably the first mechanism occurred. Indeed, Figure 1F, which provides the XRD patterns of CTAB and V_2O_5 powders and of V_2O_5 + CTAB mesoporous material, reveals that the latter had a structure similar to that of the CTAB powder. The equal distance between the XRD peaks of the CTAB powder indicates a lamellar structure. Because of the high concentration of CTAB in the solution used to prepare this mesoporous material (∼100(CMC)), it is likely that lamellar aggregates of CTAB were present, within which the vanadium species polymerized to generate the mesostructure. However, when the amount of surfactant is small, the ion pairs are expected to be involved in the self-assembly process.

We will try now to provide possible explanations for some of the experimental results obtained, namely why for a pH in the acidic range a fibrous morphology was generated, why the amount of magnesium included in the prepared material was low and that of vanadium large, and why the binary surfactants provided better materials than the single ones.

In solution, vanadium is present as polyvanadate anions of different polymerization degrees and charges, dependent on the pH.[37] Under alkaline conditions, the vanadate anions have a low degree of polymerization, and there is an equilibrium between the species VO_4^{3-}, HVO_4^{2-}, $H_2VO_4^-$, $V_2O_7^{4-}$, $HV_2O_7^{3-}$, $V_3O_9^{3-}$, and/or $V_4O_{12}^{4-}$. Under acidic conditions, the equilibrium between the polyvanadate anions involves mainly the decavanadates, $V_{10}O_{28}^{6-}$. $HV_{10}O_{28}^{5-}$, and $H_2V_{10}O_{28}^{4-}$, which have a higher degree of polymerization than those involved under alkaline conditions. In a previous paper,[34] in which vanadium acetylacetonate ($V(acac)_3$) was employed as the source of vanadium and the preparation was carried out under basic conditions, no fibrous morphology was observed for the obtained lamellar structures. The higher degree of polymerization of the polyvanadate anions in acidic media appears to be associated with the formation of a fibrous morphology.

The amount of vanadium included in the mesoporous materials was much higher than that of magnesium probably because of the strong attractive interactions between the decavanadates and the surfactant molecules (both attractive electrostatic interactions because of the opposite charges of the two species and van der Waals attractive interactions) and relatively strong repulsive interactions between Mg^{2+} and the surfactant molecules that have the same charges. The amount of magnesium increased when the mixture CTAB + HDA was employed probably because of somewhat weaker attractive interactions between HDA and decavanadates than between CTAB and the decavanadates species.

The surface area of the headgroup, a_0, is smaller for HDA than for CTAB. For this reason, the ratio $V_H/l_c a_0$ (where V_H is the volume of the hydrophobic group and l_c is its length), which determines the nature of the surfactant aggregates,[38] increases and a lamellar structure, for which the above ratio should be between $^1/_2$ and 1, becomes more likely. This may explain why, for all binary mixtures involving HDA, lamellar structures have been observed.

The higher stability of the materials prepared with CTAB + HAD than that of those prepared with CTAB alone might be due to the higher amount of magnesium present in the former case.

4. Conclusion

Lamellar mesoporous V−Mg−O could be synthesized by using V_2O_5 and $MgCl_2$ as sources and a number of surfactants as templates. The successful surfactants included the single surfactants Triton X-100, the quaternary ammonium surfactants possessing long alkyl chains, such as cetylpyridium bromide (CPB) and cetyltrimethylammonium bromide (CTAB), as well as binary mixtures composed of a quaternary ammonium surfactant and hexadecylamine (HDA). The nonionic surfactant Triton X-100 templated a mesoporous V−Mg−O with a highly ordered lamellar structure but a particulate morphology. In contrast, the cationic quaternary ammonium surfactants, particularly CTAB, and the binary mixtures consisting of a quaternary ammonium surfactant and HDA templated lamellar mesoporous V−Mg−O with a fibrous morphology. The binary mixtures of surfactants were much more effective than the single surfactants in templating a mesostructured V−Mg−O. The specimens prepared with binary surfactants were more stable during the thermal removal of the surfactants than those prepared with single surfactants.

CM020127I

(37) Kepert, D. L. In *The Early Transition Metals*; Academic Press: London and New York, 1972; pp 181.

(38) Rosen, M. J. In *Surfactants and Interfacial Phenomena*, 2nd ed.; John Wiley & Sons: New York, 1988; pp 133.